

EMI Risk Estimation for System-Level Functions Using Probabilistic Graphical Models

Lokesh Devaraj
HORIBA MIRA Limited
Nuneaton, UK

lokesh.devaraj@horiba-mira.com

Alastair R. Ruddle
HORIBA MIRA Limited
Nuneaton, UK

alastair.ruddle@horiba-mira.com

Alistair P. Duffy
De Montfort University
Leicester, UK
apd@dmu.ac.uk

Abstract—In general, the functions provided by complex systems often involve multiple sub-systems and components that are functionally dependent on each other. The dependency could be to receive power, control signals, input data, memory storage, feedback etc. With the increasing use of electronic systems to perform critical functions, the potential for malfunctions due to electromagnetic interference need to be identified and mitigated. Hence, a risk analysis, estimating the likelihood and severity of electromagnetic interference effects, is desirable from the very early stages of system development. In this paper, the use of probabilistic graphical models for estimating the likelihood of electromagnetic disturbances causing system malfunctions with various degrees of severity is demonstrated using a very simple case study. Statistical data are synthesised to illustrate the construction of conditional probability distribution tables for a Bayesian Network system model. Factorization and inference techniques are then applied to demonstrate the formulation and answer of queries that could be of value during system risk assessment.

Keywords— risk analysis, probabilistic graphical models, Bayesian network, failure analysis, electromagnetic interference.

I. INTRODUCTION

In the current practice of electromagnetic compatibility (EMC) in relation to road vehicles, the immunity testing conditions (i.e. frequency range and steps, field strength, exposure time, illumination direction, operational state etc.) are prescribed by regulatory standards. Some manufactures verify the immunity of their systems at more stringent levels for higher confidence. However, due to technical and economic limitations, it is impossible to test all possible electromagnetic interference conditions, resulting in an insufficiency of confidence due to epistemic uncertainties (i.e. things that could be known in principle, but in practice are not).

To achieve EMC for modern complex systems with rapid advancement in the features and functionality (like automated driving in road vehicles), the current industrial practice of rule-based EMC testing approach needs to be shifted, more towards a risk-based approach. As also discussed in [1], in order to accomplish a risk-based electromagnetic (EM) approach, hazards identification and risk estimation activities should commence from the initial concept phase of the system itself, and should be continuously refined as more and more system knowledge is obtained.

In [2], some of the risk factors to be considered to determine the risk parameters (likelihood and severity) for a

system-level EM risk analysis are given. This includes estimation of the likelihood of EM interference (EMI) having an impact with a particular severity level for any system function, reflecting the functional dependence or interaction between the various components that are involved. The level of risk then depends on the severity of the consequences and the likelihood of their occurrence [3]. In this paper, the application of a probabilistic graphical model (PGM) for EMI risk analysis is illustrated by considering EMI to be a common-cause of failure for multiple components performing a system function. This analysis is carried out using a Bayesian network (BN) [4]. The significant increase in the application of BN models for risk analysis and dependability for complex systems is evident from [5]. However, there is very little literature on the application of PGMs for EM risk analysis considering EM interference to be a common-cause failures and cascading failures [6].

This paper provides a simple demonstration of system-level EMI risk estimation with PGMs, using a case study consisting of functionally dependent components as discussed in Section II. Further, the details of the EMI analysis procedure and results obtained for the impact analysis and risk estimation are given in Section III-IV. Integration of the simulation results to construct the conditional probability distribution (CPD) tables of the Bayesian network model and relevant inferences obtained therefrom are discussed in Section V. The merits and limitations of PGMs for EM risk analysis are summarised in Section VI. Finally, the conclusions and related future work are summarized in the last section. In addition, the Appendix provides some further details of derivation of the EMI probability distributions.

II. SIMPLE CASE STUDY

A complex system usually employs more than one component or subsystem (comprising sensors, controllers and actuators) to perform a system function. EMI that is present in the system environment can cause malfunctions by affecting more than one component, resulting in a common-cause failure. Additionally, due to functional dependence, any erroneous signal provided by one component/subsystem could be further passed to its dependent components/subsystems, causing much severe consequences at a system level [7].

For the purposes of this study, it is imagined that a hazard analysis has been carried out and a critical system function has been identified that depends on particular data signals that are at risk from possible corruption by EMI. Although errors of up to 20% in value of the parameter carried by these signals are tolerable, differences of 20–60% would be a nuisance and anything more than 60% is considered to be unacceptable. In order to assess the associated risk, it would be desirable to estimate the probability of EMI-induced errors reaching the identified severity levels.

The research leading to these results has received funding from the European Union's Horizon 2020 research and innovation programme under the Marie Skłodowska-Curie grant agreement No 812790 (MSCA-ETN PETER). This publication reflects only the authors' view, exempting the European Union from any liability. Project website: <http://etn-peter.eu/>.

The critical data is assumed to be processed by a simple sub-system comprised of components C1 and C2 (for data transmission), and subsystems S1 and S2 (data processing) as shown in Fig. 1, is taken as an example to apply the BN model for analysing the likelihood of common-cause and cascaded failures due to EMI. The system model is based on the assumptions below.

- The *system function* is to deliver a pulse width modulated (PWM) representation of a sinusoid of frequency F to subsystem S2, where F is initially supplied as a digital signal to C1.
- Any deviation to the frequency of the sinusoidal wave reconstructed from the PWM wave by S2 is considered a *malfunction*.
- Subsystem S1 receives a numerical value transmitted via cable C1 in the form of a digital signal m_1 .
- A sinusoidal signal with frequency equal to the received numerical value is then converted to a PWM wave m_2 by S1 and transmitted through C2 to subsystem S2.
- For the purposes of this case study, S1 and S2 are assumed to be immune to the EMI applied for the analysis, whereas C1 and C2 are both considered to be potentially susceptible to the EMI.

Component C2 is therefore functionally dependent on C1, as the frequency of the PWM signal transmitted through C2 is based on the value received by S1 from C1.

Assuming PWM modulation and demodulation functions denoted by $Pwm(m_j)$ and $Ipwm(m_j)$, respectively, are applied to a signal m_j , then the modulated signal $m_2 = Pwm(m_1)$ corresponds to a sinusoid of frequency F if C1 is unaffected by EMI. Furthermore, if C2 is also unaffected by EMI then the demodulated signal $Ipwm(m_2)$ has a frequency equal to F . However, if either or both signals are affected by EMI then a malfunction, where $Ipwm(m_2) \neq F$, is a possible outcome.

III. LIKELIHOOD ESTIMATION FOR EMI

To emulate the susceptibility of C1 and C2 to EMI noise, continuous sinusoids of the form $N_k = A_k \sin(2\pi f_k t + \varphi_k)$ were added to the cable signals m_1 and m_2 . A total of 6262 random noise samples were derived, with uniform distributions over the ranges allocated for the amplitude A_k (1 to 1.5 V), the frequency f_k (15 kHz to 0.3 MHz), and the initial phase φ_k (0 to 2π radians) of the noise.

A. Generating Signals for C1 and C2

The signals m_1 and m_2 that are transmitted through cables C1 and C2, respectively, are generated as outlined below.

1. The intended target value, F , is converted to a digital signal in binary format (0 = -1 V and 1 = +1 V), with a bit rate of 100 kbits/sec. For a target value $F=150$,

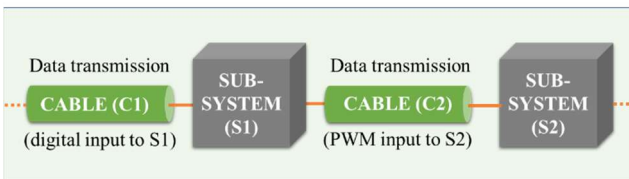


Fig. 1 System model considered for casestudy: sub-system S1 transmits input data (digital) through cable C1, which is processed by sub-system S2 to provide the output data (PWM wave) through cable C2.

the digital input to cable C1 corresponds to 10010110.

2. Where required, EMI may be added to the signal m_1 .
3. Using an intersective method (a sawtooth waveform was used as the modulating waveform), a PWM pulse train is constructed as the input to C2, corresponding to a sinusoidal signal with frequency equal to the value (in kHz) received by subsystem S1 in the form of m_1 .
4. Where required, EMI may be added to the signal m_2 .
5. The PWM pulse train that is transmitted via C2 is demodulated by S2 to retrieve the frequency of the sinusoid represented by m_2 .

Signals were generated for three EMI conditions, with EMI applied individually to m_1 (denoted E_1) and m_2 (E_2), as well as applied to both m_1 and m_2 concurrently (E_3).

B. Probability of Malfunction

If the frequency decoded by S2 under EMI condition E_n is $G_k(E_n)$, then the corresponding relative deviation $D_k(E_n)$ from the target value F is obtained from:

$$D_k(E_n) = 100 \left| \frac{G_k(E_n) - F}{F} \right| (\%) \quad (1)$$

The decoded frequency values $G_k(E_n)$ were obtained by selecting the highest peak (Pk) of the Fourier transform (Ft) of the signal demodulated by S2 for the three potential EMI conditions:

$$G_k(E_1) = \text{Pk}\{\text{Ft}\{Ipwm\{Pwm(m_1 + N_k)\}\}\} \quad (2)$$

$$G_k(E_2) = \text{Pk}\{\text{Ft}\{Ipwm\{Pwm(m_2) + N_k\}\}\} \quad (3)$$

$$G_k(E_3) = \text{Pk}\{\text{Ft}\{Ipwm\{Pwm(m_1 + N_k) + N_k\}\}\} \quad (4)$$

The results of relative deviations due to EMI in C1 (2), C2 (3), and C1 and C2 concurrently (4) were obtained by adding the 6262 EM noise samples for each of the three cases. The data collected was used to generate the cumulative distribution functions (CDFs) for EMI that are illustrated in Fig. 2, for EMI in C1, in C2, and in both C1 and C2 concurrently (denoted C1&C2). Details of the corruption of the signals m_1 and m_2 due to EMI are not key to the focus of this paper and are therefore explained in more detail in the Appendix, with relevant examples.

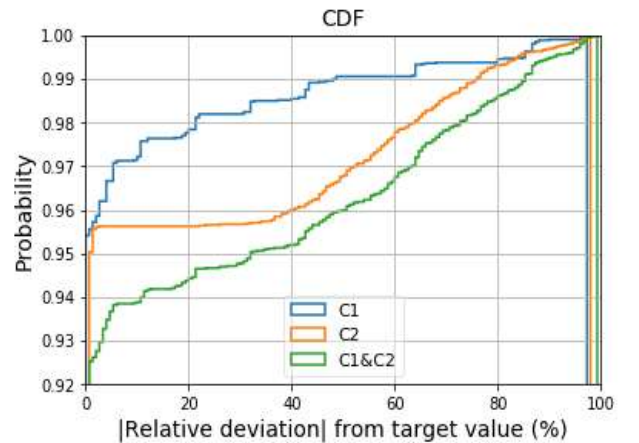


Fig. 2. Cumulative distribution functions for the deviations $D_k(E_n)$ due to EMI noise in C1, C2 and C1&C2.

IV. SEVERITY OF EMI IMPACT AND RISK

To enable estimation of the system level risk associated with the EMI, the relative deviation caused by the EMI is assumed to have varying levels of *severity* of consequences. Hence, based on the magnitude of the relative deviation, D (%) from the intended target value, the severity S of the possible malfunctions is categorized as, low (tolerable), medium (undesirable) or high (intolerable) according to:

$$S(D) = \begin{cases} \text{low} & \text{if } 0 \leq D \leq 20 \\ \text{medium} & \text{if } 20 < D \leq 60 \\ \text{high} & \text{if } D > 60 \end{cases} \quad (5)$$

Probability values for the severity levels (low, medium or high) associated with EMI effects on C1, C2, and C1&C2 are given in Table I. A comparison of these probabilities shows that it is highly likely that the EMI considered here will be of low severity for the system function by affecting components C1 and C2 independently, with the result that the associated risk levels are also low, given that the estimated probabilities for low severity impacts are very high: $P(C1 = \text{low}) = 0.9784$ and $P(C2 = \text{low}) = 0.9562$ (see Table I).

From a component supplier's perspective, having such low risks might seem to be acceptable at first sight. However, it should be noted that the probability for having the low severity outcome for the C1&C2 situation $P(C1\&C2 = \text{low})$ is smaller. This implies that, at a system-level, there is an increase in the likelihood of system malfunctions with *medium* and *high* severity, due to the functional dependence of components C1 and C2 (although in this particular example the increase is relatively small).

V. EMI RISK ESTIMATION WITH BN

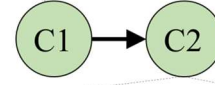
For complex systems exploiting a high proportion of electrical and electronic components to perform system functions, EMI could be a common-cause of malfunctions or failures. The estimation of risk for such systems (i.e. determining the likelihood and severity of the EMI impacts) becomes increasingly difficult as the number of system functions when using more traditional tools (such as failure mode and effects analysis, fault trees, event trees etc.), , system components, and component failure modes increases. In this section, the application of EM risk analysis with BN (a PGM) is illustrated for the simple case study considered in this paper.

A BN is a graphical structure consisting of a network of nodes representing model variables and edges representing a causal relationship between pairs of connected nodes. The functional dependence between components can be considered as a causal factor in determining the likelihood of impacts at a particular level of severity for the system function. Considering the simple case study reported here, it is possible to represent the functional dependence of C2 on C1 in delivering the system function by using the BN graph and its associated conditional probability tables (CPDs), which are illustrated in Fig. 3.

TABLE I. PROBABILITY DISTRIBUTION TABLE FOR SEVERITY OF EMI IMPACT FOR C1, C2, AND C1&C2

	<i>low</i>	<i>medium</i>	<i>high</i>
C1	0.978441	0.012137	0.009422
C2	0.956244	0.021559	0.022197
C1&C2	0.944267	0.023315	0.032418

$P(C1)$	C1 = <i>low</i>	C1 = <i>medium</i>	C1 = <i>high</i>
	0.978285	0.012135	0.00958



$P(C2 C1)$	C2 = <i>low</i>	C2 = <i>medium</i>	C2 = <i>high</i>
C1 = <i>low</i>	0.963767	0.01322	0.023013
C1 = <i>medium</i>	0.105263	0.855263	0.039474
C1 = <i>high</i>	0.016667	0.2	0.783333

Fig. 3. Simple BN representation of the functional dependence between components C1 and C2 as a causal factor to determine the probability of the degree of EMI impact on system function. Conditional distribution tables for EMI impact on C1 and C2 | C1 are given for nodes C1 and C2.

A. CPD Table Entries for BN Nodes

The estimated probability values in the CPD tables for BN shown in Fig. 3 were obtained by analysing the statistical data outlined in section III. As component C1 does not have any parent nodes, the probability distribution of $P(C1)$ is independent of any other node variables (i.e. C1 is not dependent on any other component within the system to perform the system function). Hence, $P(C1)$ is not conditional on any other node variable and is directly obtained from Table I. However, C2 is dependent on its parent node C1 and is therefore conditioned on the state space assigned to the node variable C1.

In Fig. 4, an event tree is used to illustrate the steps followed in determining the values of CPD table $P(C2 | C1)$ for node C2 in Fig. 3. It should be noted that, among the 6262 simulated noise samples initially considered for determining the CPD of EMI impact $P(C2 | C1)$, only the specific event $P(C2 = \text{low} | C1 = \text{high})$ was never observed. Assigning zero probability for a rare but possible event only because it was not observed in a samples study would be unacceptable due to its impact on related probability values. In order to overcome this situation, a Bayesian approach to estimate the probability using *equivalent sample size* is given in [9]. For the case study, no prior knowledge is available to determine the required sample size to observe this event and its probability can only be quantified as $<1/6262$. To avoid the ambiguity of assigning a zero-probability value to a possible event, it is assumed that it would be observed if noise sample 6263 were to be generated (an indication of the additional sample is given by the red circles in Fig. 4).

The CPD values of node C2 in the BN provides the likelihood of system level impact due to EM susceptibility of component C2, given each state space of the node variable C1. For instance, if the EM noise affecting component C1 caused a medium level impact, then the probability that the impact is high due to EM susceptibility of C2 is approximately 4% (see Fig. 3).

B. Joint Probability of EMI Impact Severity

As previously given in [2], if all the nodes of a BN are responsible for a system-level function, then the overall probability for the functional deviation at system-level can be determined from their joint probability distribution (JPD). In this case study, both nodes (C1 and C2) in Fig. 3 are assigned

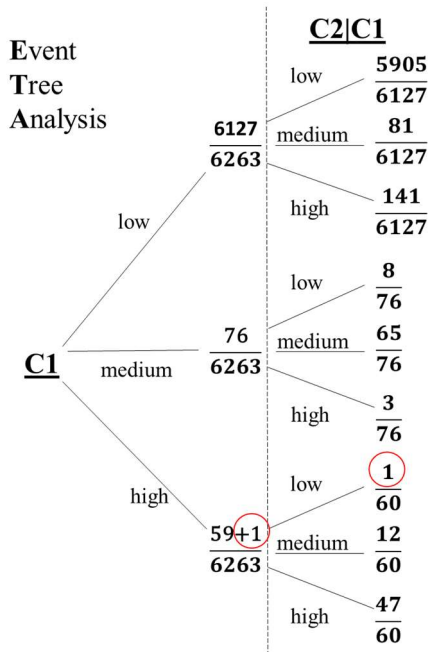


Fig. 4. An event tree to illustrate the condition probability values obtained for the CPD table in Fig. 3.

to perform the system-level function, hence the overall probability measure of system-level impact can be determined from their JPD, which is given by:

$$P(C1, C2) = P(C1|pa\{C2\}) P(C2|pa\{C2\}) \quad (6)$$

where the function $pa(X)$ represents the parents of a node variable X .

The factorization for the JPD is based on the independence properties obtained from the BN structure and the chain rule for the PGMs [9]. In this case study, $pa(C1) = \emptyset$ (i.e. the empty set) and $pa(C2) = C1$. In real-world systems there could be several components with functional dependencies that collectively implement a single system function. In such cases the BN might consist of several nodes and edges. Relevant examples of factorization for a BN with more than two nodes is given in [1], [8]. The JPD table for all possible state spaces for node variables $C1$ and $C2$ is provided in Table II.

C. Bayesian Inference and Queries

One of the main applications of BN in risk analysis is the ability to estimate the likelihood of various queries, as more evidence is available [8]. A possible query for the BN of the case study model could be “What is the probability of an intolerable (high) impact on the system due to EMI effects on $C2$, given that the EMI effects on $C1$ are tolerable (low)?”. Using conditional probability, this query can be expressed as:

$$P(C2 = high|C1 = low) = \frac{P(C1, C2)}{P(C1)} = 0.023 \quad (7)$$

TABLE II. JOINT PROBABILITY DISTRIBUTION TABLE FOR SEVERITY OF EMI IMPACT FOR $C1$ AND $C2$

$P(C1, C2)$	$C2 = low$	$C2 = medium$	$C2 = high$
$C1 = low$	0.942839	0.012933	0.022513
$C1 = medium$	0.001277	0.010378	0.000479
$C1 = high$	0.00016	0.001916	0.007504

Further inference queries related to either a single node variable or to a specific group of node variables in the BN can be answered by the method of *marginalization*, which is also known as sum-product variable elimination [4]. For the case study, the query “What is the probability of a tolerable (low) impact on the system due to EMI effects on $C2$?” can be obtained by marginalizing $P(C2 = low)$, i.e., by performing a summation of all values corresponding to the JPD column $C2 = low$ in Table II.

The JPD table values are actually the product of terms given in (6). The marginal probabilities of $C2 = low$, $C2 = medium$, and $C2 = high$ are obtained as follows:

$$\sum_{C1} P(C1) P(C2 = low|C1) = 0.944276 \quad (8)$$

$$\sum_{C1} P(C1) P(C2 = medium|C1) = 0.025227 \quad (9)$$

$$\sum_{C1} P(C1) P(C2 = high|C1) = 0.030496 \quad (10)$$

It can be seen that the independent probability values $P(C2)$ given in Table I and the marginal probability values for $P(C2)$ obtained from the Bayesian inference of (8)–(10) are different. This is because the latter consider the functional dependence of $C2$ on $C1$, facilitated by the BN. Since the case study has just two nodes in the BN model, the inferences are quick and do not necessarily need thorough mathematical formalization. In practice, however, for more realistic systems with multiple components and component failure states, a similar BN would have many nodes and edges, resulting in an exponential increase in the order of the JPD.

In such cases, some subexpressions in the joint distribution that need be estimated for specific probability queries depend on a small number of variables, according to the independencies provided by the BN structure [4], [7]. Other inference techniques such as *maximum a posteriori* (MAP) inference can be further used during the risk management process to find the single highest probability. In the current analysis, a MAP query could be “What is the probability value for the most likely impact severity class due to EMI effects on $C2$ given that EMI effects on $C1$ ’s are intolerable?”. From the CPD table of Fig. 3 for node $C2$, it can be seen that the highest probability value given that $C1$ is *high* is 0.78, which occurs when $C2$ is also *high*. The mathematical formulation of MAP queries for complex system is described in [4].

VI. MERITS AND LIMITATIONS OF PGMs IN RISK ANALYSIS

Risk analysis for complex systems (including road vehicles, aircraft, ships etc.) involves multiple system functions, components and failure states. For such systems, risk analysis with PGMs like BN and Markov Random Fields [10] provide better handling of the system complexity, through graphical visualization of the system components/subsystems together with their functional dependence in a single model.

Some of the advantages of using PGMs over the traditional risk analysis tools such as event tree analysis (ETA) and fault tree analysis (FTA), for risk estimation include the following.

1) The structures of fault trees and event trees are unidirectional, with the result that analysing common cause failures with bidirectional functional dependencies between

components would require multiple tree structures for a single system. Using PGMs, however, bidirectional functional dependencies can be represented in a single system model.

2) Compact representations of complex distributions, mathematical formalizations for inference tasks, and software tools for PGM realization, can support the decision-making process by making these process be more efficient and less time consuming.

3) Other technical and non-technical aspects relating to a component that may influence its EM susceptibility (such as component location within the system, shielding effects due to surrounding structures, EMI detection measures etc.) may also be added as additional nodes to the PGM structure. Further details on this are provided in [8].

The limitations of BN include modelling and computing difficulties as the number of parents associated with any single node in the model increases. For example, if a component X depends on ten other components or node variables, then the CPD table for node X would have $2^{10} = 1024$ entries. This would be a difficult task for an expert to perform, without access to sufficient data. In such cases, however, possibility theory or fuzzy logic could be employed to assign the CPD values [1]. Also, BNs belong to a class of PGMs having directed acyclic graph structures. Thus, BNs are unable to represent functional dependencies involving feedback loops. A possible solution to this limitation is to employ another class of PGMs called Markov random fields, which are graphs with undirected cyclic structure [10], thereby permitting feedback loop type dependencies. Another potential solution (although with increased complexity) is to employ dynamic BNs, which are temporal PGMs, modelled in time-slices [4].

VII. CONCLUSIONS AND FUTURE WORK

For complex systems, estimating the risk of EMI impact on the system functions involves considerable epistemic uncertainty arising from the lack of detailed system knowledge. Moreover, EMI being a common cause of failure, it can simultaneously affect more than one component or subsystem, with the potential to cause even more severe system-level consequences due to the functional dependence between the affected components and/or subsystems.

In this paper, representative probabilistic data relating to EMI impact was generated using very simple methods in order to allow the CPD entries for a very simple BN model to be constructed for the case study outlined in Section II. In practice, however, such data could be derived from more realistic and detailed physical measurements or numerical simulations, or a mix of measurements and simulations.

This synthetic data allowed the identification of the severity of the system-level consequences, and hence estimation of the EMI-related risk, to be illustrated for a very simple system with some functional dependence. In addition, this data allowed the demonstration of various inference techniques that could be used to formulate and answer probability queries that would help to support system risk assessments.

Future work will further extend and develop the use of PGMs for system risk analysis, such as combining data obtained from measurements and/or simulations with the influence of non-technical factors on the key risk parameters (likelihood and severity). In addition, related automotive applications, such as communications system performance, will be investigated using this type of analysis.

APPENDIX – GENERATION OF STATISTICAL DATA

Firstly, it should be noted that the EMI probability distributions used in this work reflect neither the detailed physics of EMI nor the practical methods used to mitigate EMI effects, both of which are outside the scope of this paper. The results described here are purely synthetic and solely for the purposes of providing a representative source of statistical data for illustrating the use of PGM methods that are the subject of this paper.

Determining the likelihood of EMI in components C1 and C2 having a particular severity of system level impact involves determining the probability and magnitude of the deviation from the intended output due to EMI noise in signals m_1 and m_2 . This Appendix details of details the determination of $G_k(E_1)$ and $G_k(E_2)$ that are used for calculating the relative deviations $D_k(E_1)$ and $D_k(E_2)$ of Section III.B with reference to a specific target value, $F = 150$, and with a particular EMI noise example N_a (with amplitude 1.38 V, frequency 20.58 kHz and phase 5.5 radians) affecting C1 and/or C2.

A. EMI Condition E_1 ($m_1 + N_a$)

Addition of noise to signal m_1 (i.e. affecting C1 only) is considered as the first potential EMI condition, E_1 (see Section III.B). In practice it is not actually necessary to include the PWM modulation and demodulation as indicated in (2) since it is assumed that C2 is not affected by EMI in this case.

The digital signal m_1 , obtained by converting the target value $F = 150$ to a rectangular pulse-train in binary format corresponding to ‘10010110’ as shown by the *input* in Fig. 5(a). The noise signal N_a is then simply added to the

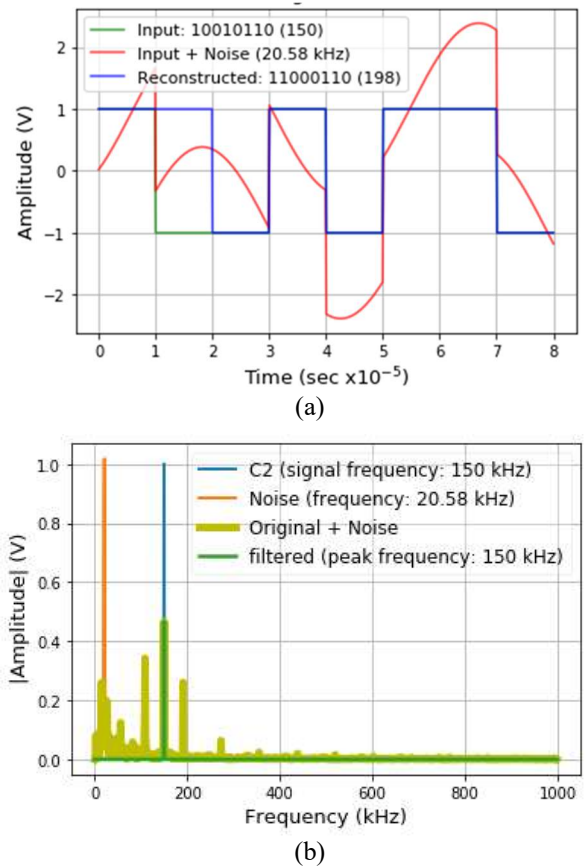


Fig. 5. Original and corrupted signals (due to noise sample N_a) for EMI conditions (a) E_1 and (b) E_2 .

signal m_1 to obtain the *input + Noise* waveform in Fig. 5(a). It can be observed that the addition of noise completely disrupts the intended signal. Nevertheless, for the purpose of calculating the deviation, the noisy signal was assumed to be reconstructed and decoded at S1. To reconstruct the noisy signal, the *mean* amplitude value over one-bit time interval (10^{-5} s) is compared to 0 V. If the *mean* > 0 V then the bit value is +1 V, otherwise it is considered to be -1 V. The reconstructed 8-bit signal for $(N_a + m_1)$ is '11000110' which corresponds to a decimal value of 198. So, for this example, using (1), the relative deviation $D_a(E_1)$ from the intended target value (150) is 32%.

B. EMI Condition E_2 ($m_1 + N_a$)

Similarly, to condition E_1 , the addition of noise to PWM signal m_2 (modulated based on a sinusoid of target frequency 150) is considered as the second EMI condition E_2 . The steps to calculate of the deviation from target frequency is given below:

- 1) Generate a sinusoid of frequency $F = 150$ kHz and then convert it into a PWM signal $m_2 = \text{Pwm}(150)$, shown in Fig. 6(a).
- 2) Add noise N_a to signal m_2 , as illustrated in Fig. 6(b).
- 3) Demodulate the corrupted signal $(N_a + m_2)$ to obtain the demodulated signal $\text{Ipwm}(N_a + m_2)$, which is shown in Fig. 6(c).
- 4) Estimate the sinusoidal signal from the demodulated noisy PWM signal $(N_a + m_2)$ by selecting the highest peak from the Fourier transform of the demodulated signal $\text{Ipwm}(N_a + m_2)$.
- 5) Determine the difference between the frequency value obtained from this process and the original target frequency of 150 kHz.

For this example, the noise waveform (N_a) yields a relative deviation $D_a(E_2) = 0$.

C. EMI condition E_3 ($E_1 + E_2$)

In EMI condition E_3 , condition E_1 is first applied to signal m_1 and then the decoded value is subjected to PWM modulation before the application of EMI condition E_2 . The resulting difference $D_a(E_3)$ is then obtained from the peak of the Fourier transform of the demodulated signal received at S2, as indicated in (4).

REFERENCES

[1] L. Devaraj, A. R. Ruddle and A. P. Duffy, "System level risk analysis for immunity in automotive functional safety analyses," Proc. 2020 International Symposium on Electromagnetic Compatibility - EMC Europe 2020, Rome, Italy, 2020.

[2] L. Devaraj, A. Ruddle, A. Duffy, "Electromagnetic risk analysis for EMI impact on functional safety with probabilistic graphical models and fuzzy logic," IEEE Letters on Electromagnetic Compatibility Practice and Applications, vol. 2, No. 4, December 2020, pp. 96–100.

[3] E. Genender, H. Garbe and F. Sabath, "Probabilistic risk analysis technique of intentional electromagnetic interference at system level," IEEE Trans. Electromag. Compat., vol. 56, (1), pp. 200–207, 2014.

[4] D. Koller and N. Friedman, Probabilistic Graphical Models: Principles and Techniques, MIT Press, London; Cambridge, Massachusetts, 2009.

[5] P. Weber et al, "Overview on Bayesian networks applications for dependability, risk analysis and maintenance areas," Engineering Applications of Artificial Intelligence, vol. 25, (4), pp. 671–682, 2012.

[6] S. Yang et al, "Study on the EMI impact over the safety of railway signaling and case analysis," 2017 2nd International Conference on System Reliability and Safety, vol. 2018, pp. 374–379, Milan, Italy, Dec. 2017

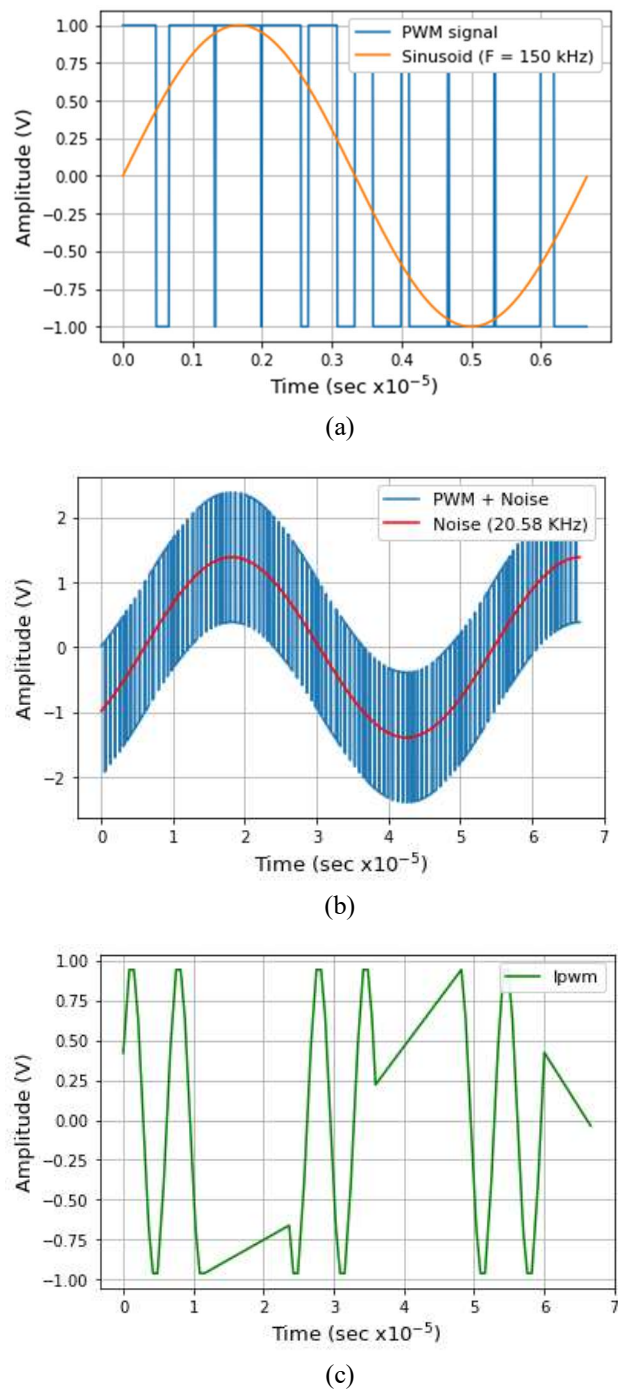


Fig. 6. Example plots to illustrate steps considered in EMI condition E_2 : (a) target frequency F and $\text{Pwm}(F)$ waveform; (b) noise N_a and waveform $\text{Pwm}(F)+N_a$; and (c) demodulated noisy waveform $\text{Ipwm}(\text{Pwm}(F)+N_a)$

[7] N.G. Leveson, Engineering a Safer World – Systems Thinking Applied to Safety, MIT Press, Cambridge, MA, 2011.

[8] L. Devaraj, A. R. Ruddle, A. P. Duffy and A. J. M. Martin, "Risk-assessment approach for EM resilience in complex systems using Bayesian Networks," Proc. 2021 Joint IEEE Int. Symp. Electromag. Compat., Signal & Power Integrity, EMC Europe 2021, Sept. 2021.

[9] A. Freno and E. Trentin, Hybrid Random Fields: A Scalable Approach to Structure and Parameter Learning in Probabilistic Graphical Models, Intelligent Systems Reference Library Vol. 15, Springer-Verlag, Berlin, ISBN 978-3-642-20307-7, pp. 28–33, 2011.

[10] Wainwright M J, Jordan M I (2008), "Graphical models, exponential families, and variational inference," in Foundations and Trends in Machine Learning, vol. 1, Nos. 1–2, pp. 1–13.